

Beam Dynamics in a Long-Pulse Linear Induction Accelerator

Carl Ekdahl, for the DARHT team

Los Alamos National Laboratory

Presented at

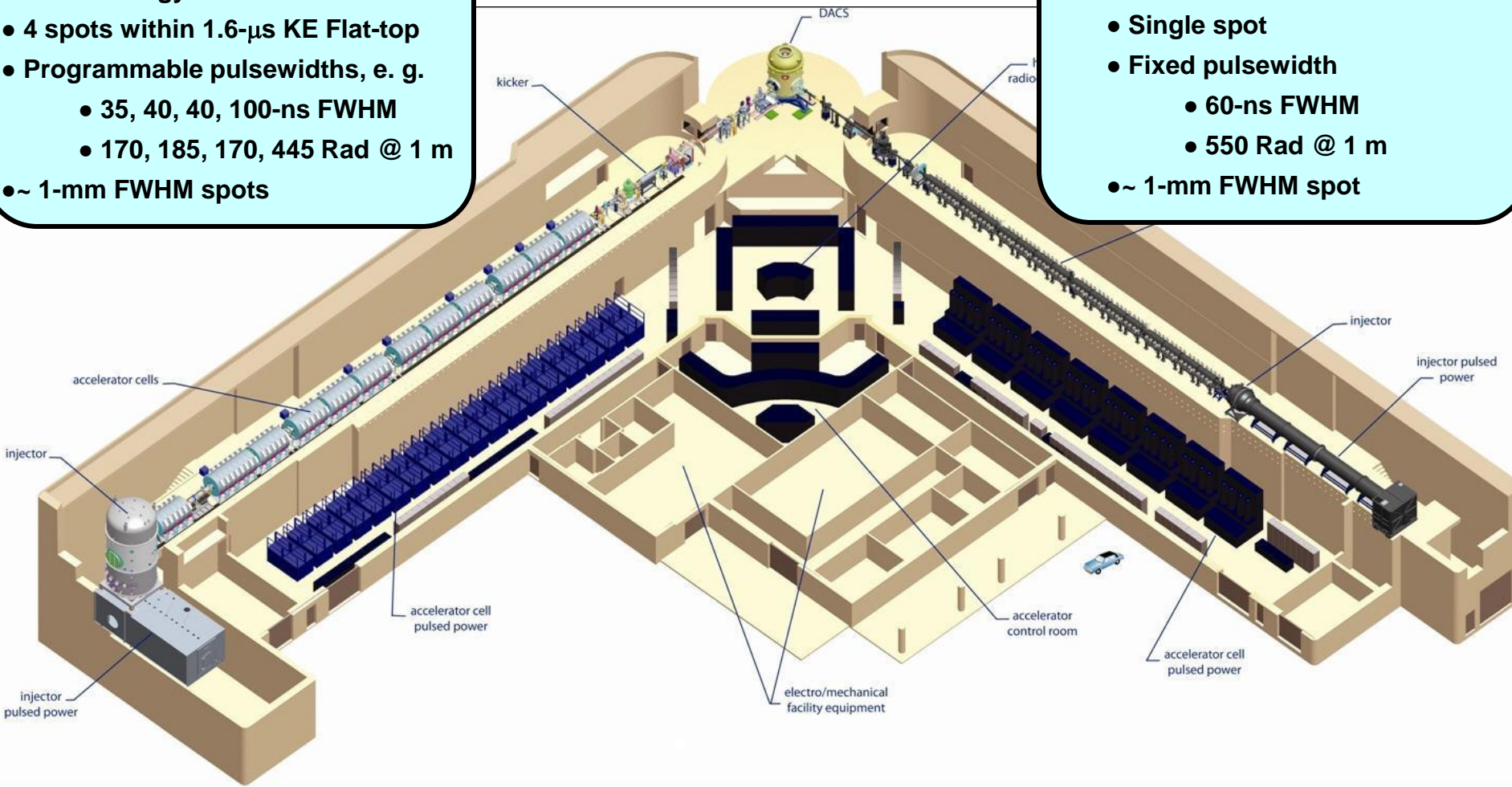
EAPPC-Beams 2010

October 13, 2010

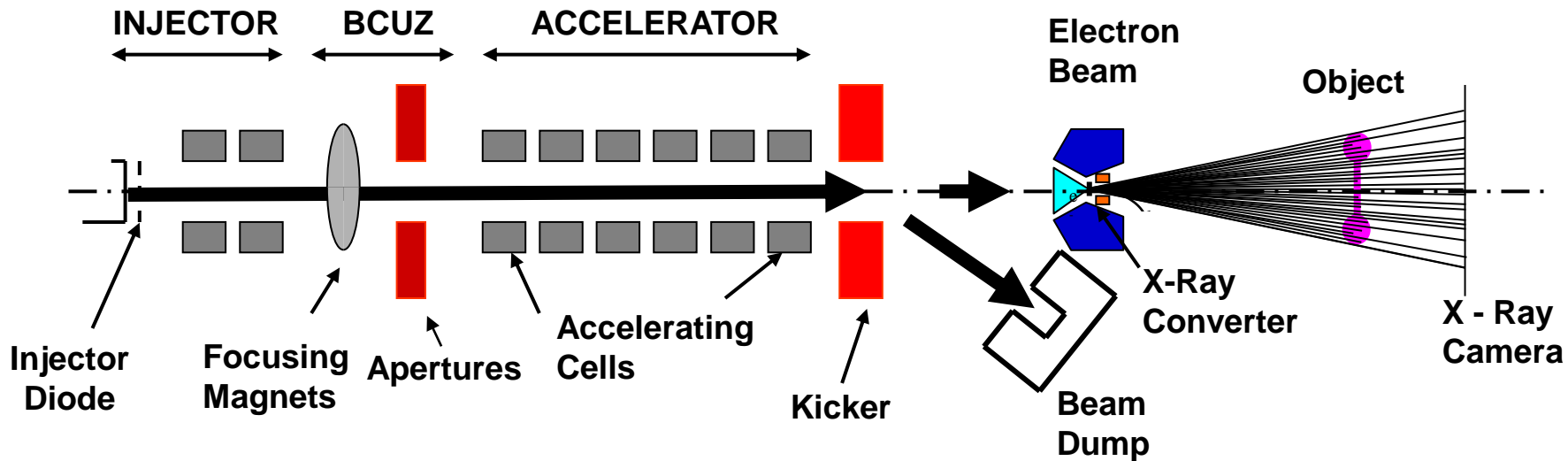
The Dual-Axis Radiographic Hydrodynamic Testing (DARHT) facility uses two linear induction accelerators (LIAs) to obtain orthogonal views of fully contained hydrodynamic tests at multiple times.

- Axis 2, Completed 2008
- Beam Energy = 16.5 MeV
- 4 spots within 1.6- μ s KE Flat-top
- Programmable pulsewidths, e. g.
 - 35, 40, 40, 100-ns FWHM
 - 170, 185, 170, 445 Rad @ 1 m
- ~ 1-mm FWHM spots

- Axis 1, Completed 1999
- Beam energy = 19.8 MeV
- Single spot
- Fixed pulsewidth
 - 60-ns FWHM
 - 550 Rad @ 1 m
- ~ 1-mm FWHM spot



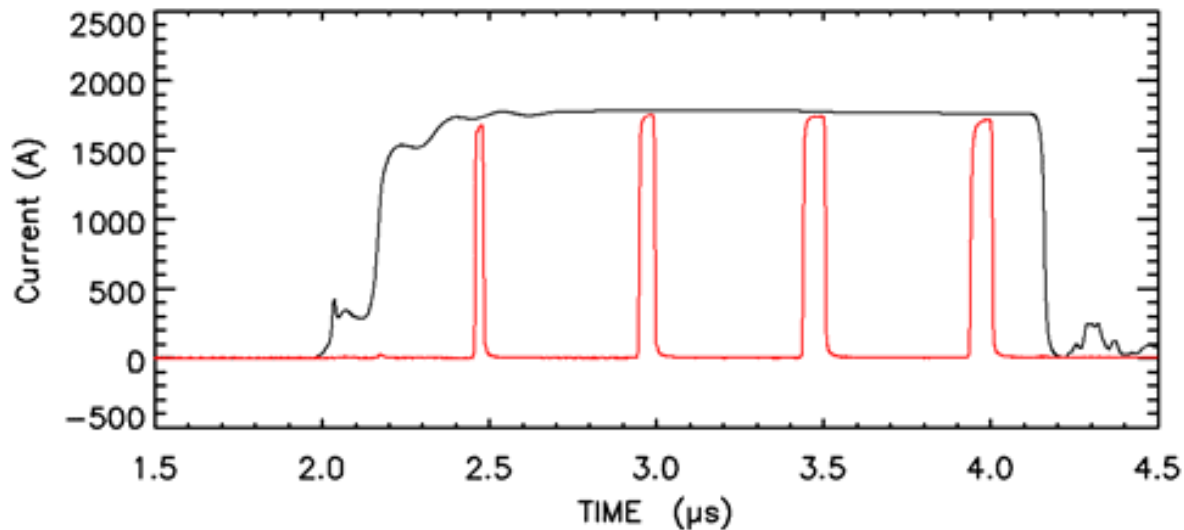
The second axis of DARHT produces multiple pulses for time resolution of hydrodynamic tests. This is a significant advance in hydrotest radiography technology.



Axis-2 accelerates a 1.8-kA, 2- μ s FWHM pulse to 16.5 MeV.

A high-speed kicker slices out multiple micro-pulses.

The micro-pulses are converted to bremsstrahlung for radiography.



We have a significant effort to understand and reduce beam motion in the DARHT axis-2 accelerator, because beam motion would be a problem for the multiple-time radiographic source spots.

- **In this talk I will discuss two examples:**
 - **Fast motion, on a ns time scale, would enlarge the source spots through time-integrated blurring.**
 - For example, we suppress the beam-breakup (BBU) instability through accelerator construction features and by tuning the magnetic focusing fields.
 - **Slow motion, on a μs time scale, would produce spot-to-spot displacement.**
 - For example, we minimize the beam sweep caused by the accelerator architecture and pulsed power by tuning magnetic dipole-corrector fields.

Large amplitude, high frequency motion due to the beam breakup (BBU) instability would enlarge our spot sizes by time integrated blurring.

- Beam breakup (BBU) plagues all electron linear accelerators, and is especially troublesome for high current linear induction accelerators.
- BBU results from beam coupling of accelerating-cell TM_{1n0} cavity modes.
- There is no stability threshold, so BBU can only be suppressed, not eliminated.
- In the high-current, strongly-focused, accelerated-beam regime of DARHT, the BBU instability rapidly grows to a maximum amplitude and then saturates due to cavity losses.

- The maximum amplification is:

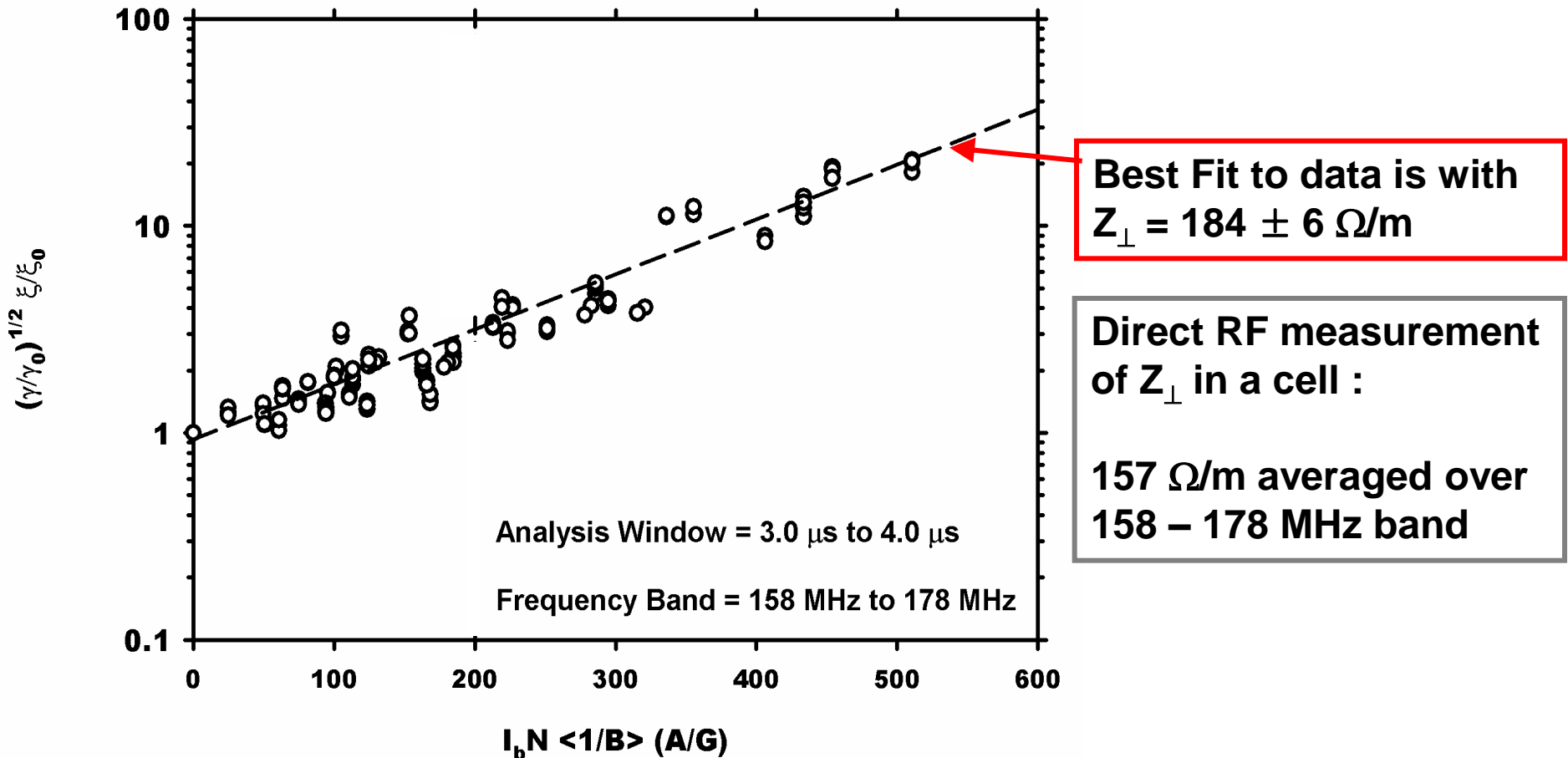
$$\xi(z)/\xi_0 = (\gamma_0/\gamma)^{1/2} e^{\Gamma} ; \text{ where } \Gamma = I_b N_G Z_{\perp} \langle 1/B_Z \rangle / 3E4$$

- In axis-2, the BBU amplitude reaches this maximum in a short time:

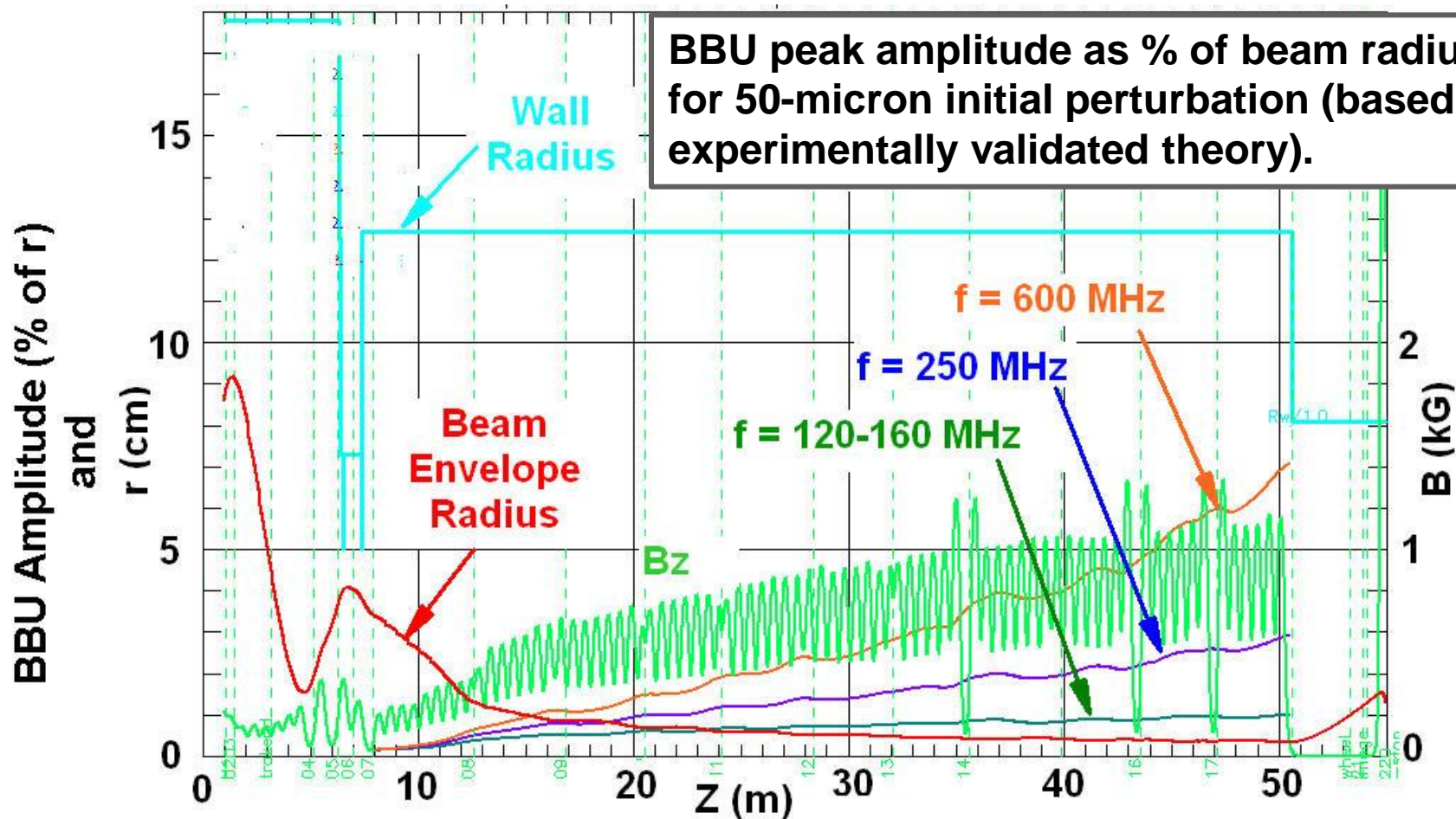
$$\tau = (2Q/\omega)\Gamma < 25 \text{ ns}$$

- ★ The accelerating cells incorporate ferrite tiles to reduce Z, thus reducing the maximum amplitude of BBU growth.

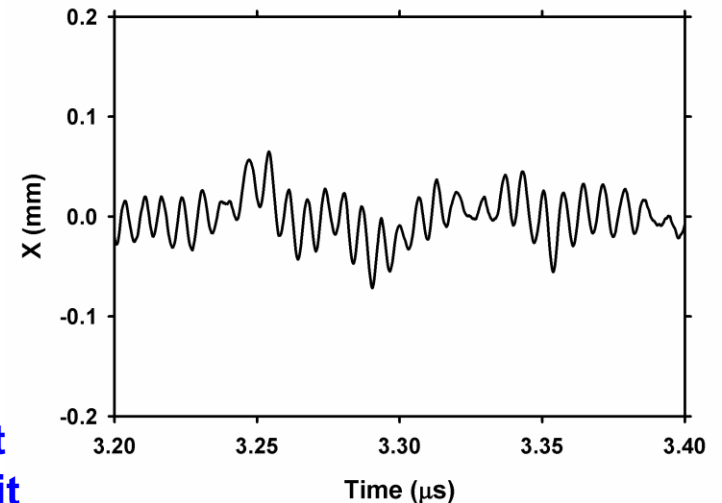
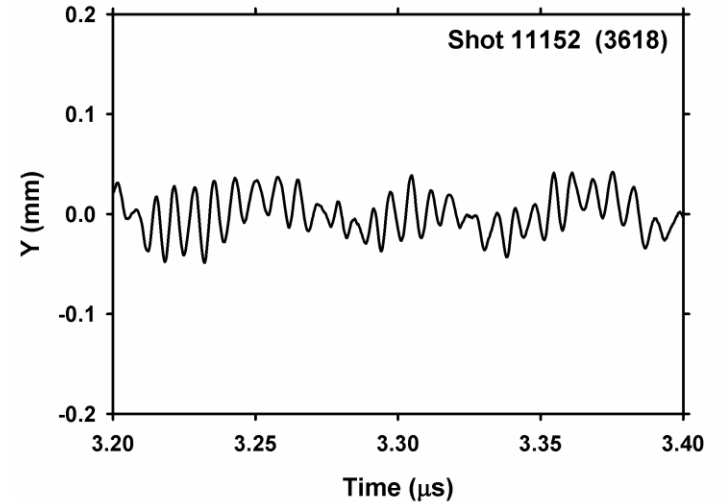
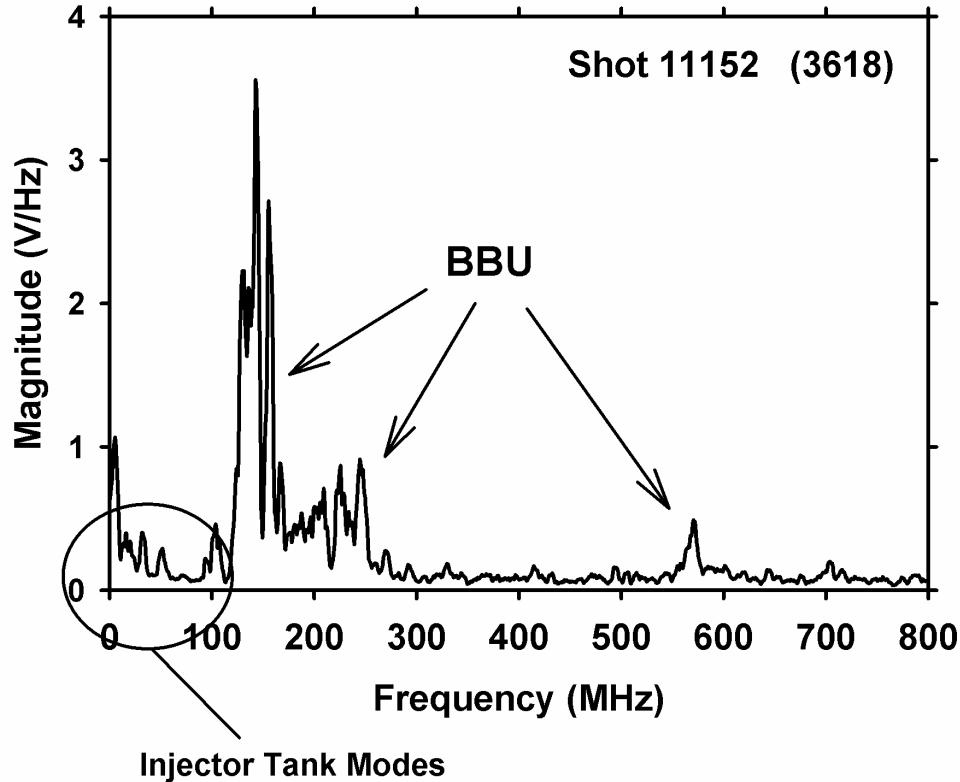
We confirmed the theoretical scaling of BBU growth for strongly-focused, high-current, accelerated beams in experiments with an early configuration using 50 accelerator cells (2005).



Based on the experimentally validated theory, the design of the final tune was predicted to be very robust to the BBU instability, because of the strong magnetic field.



Low level BBU is present at all of the resonant frequencies of the cells. However, amplitudes are $< 2\%$ of the expected beam radius ($R > 5$ mm).



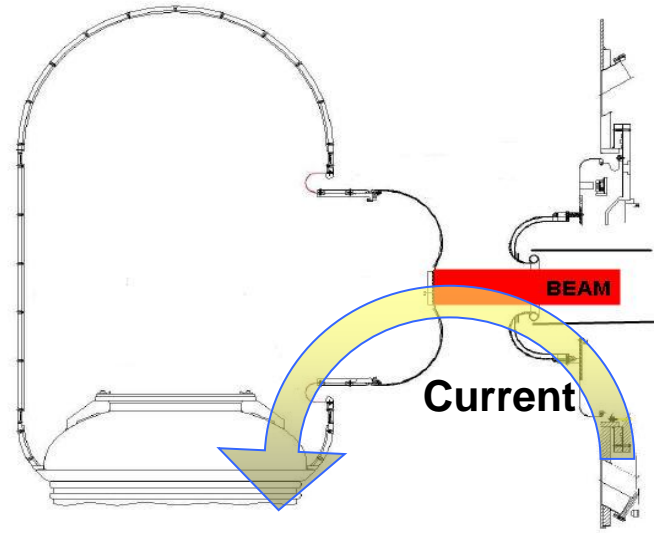
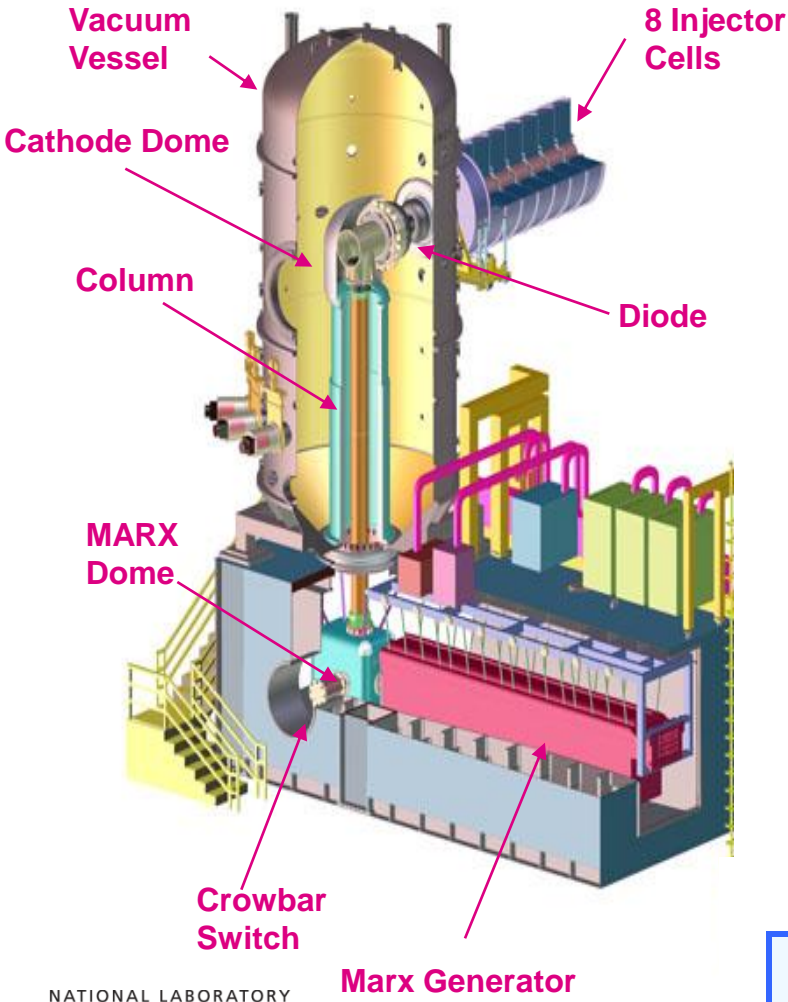
Beam envelope simulations predict beam radius $\sim 5 - 10$ mm at the exit

We have spent a significant effort to understand and reduce beam motion in the DARHT axis-2 accelerator, because beam motion would be a problem for the multiple-time radiographic source spots.

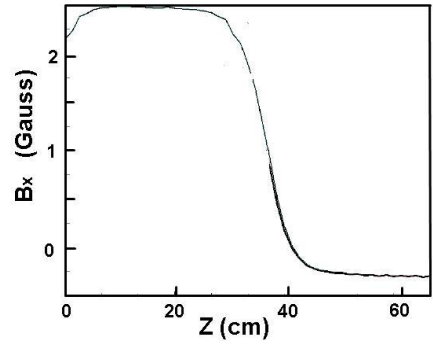
- **In this talk I will discuss two examples:**

- Fast motion, on a ns time scale, would enlarge the source spots through time-integrated blurring.
 - For example, we suppress the beam-breakup (BBU) instability through accelerator construction features and by tuning the magnetic focusing fields.
- **Slow motion, on a μs time scale, would produce spot-to-spot displacement.**
 - For example, we minimize the beam sweep caused by the accelerator architecture and pulsed power by tuning magnetic dipole-corrector fields.

A folded current path to the beam-generating diode resulted from space constraints of fitting the LIA into the building.



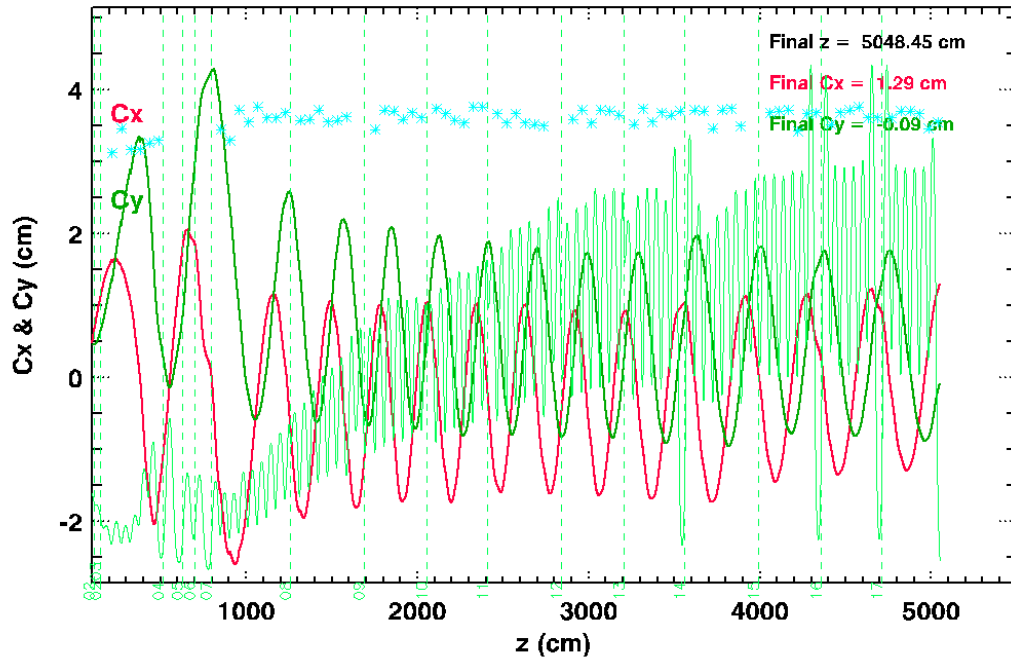
The asymmetric current path produces a transverse magnetic field in the diode.



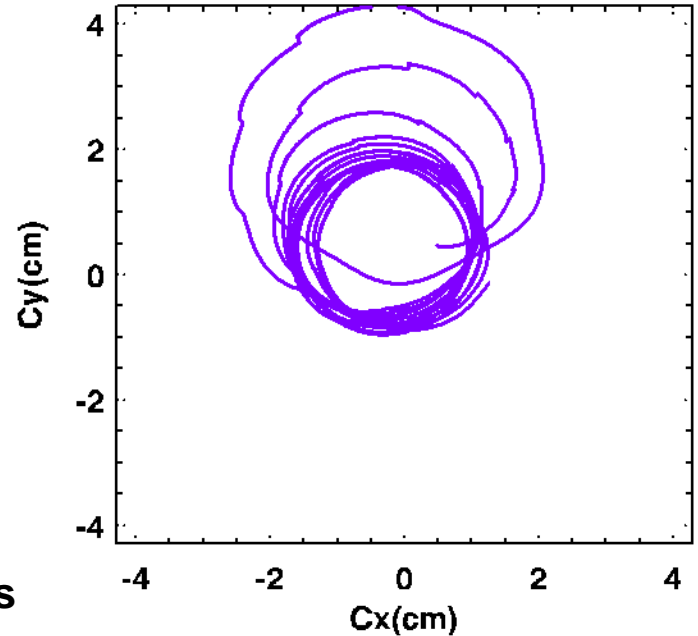
The transverse field deflects the beam upward

The solenoidal focusing field is nulled at the cathode by a bucking coil, so the upwardly deflected beam injected into the increasing solenoidal field causes a helical beam trajectory through the accelerator.

For a constant beam kinetic energy, the helix is stationary in time.



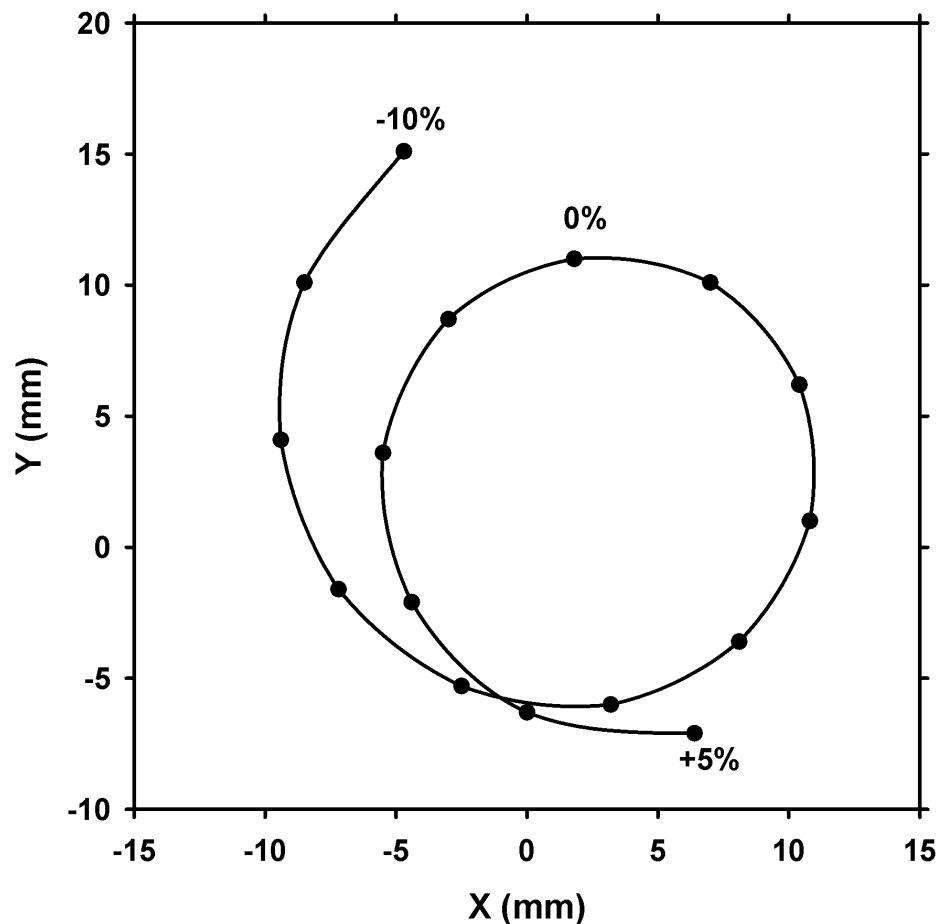
Side view of the trajectory showing X and Y positions



End-on view of the trajectory

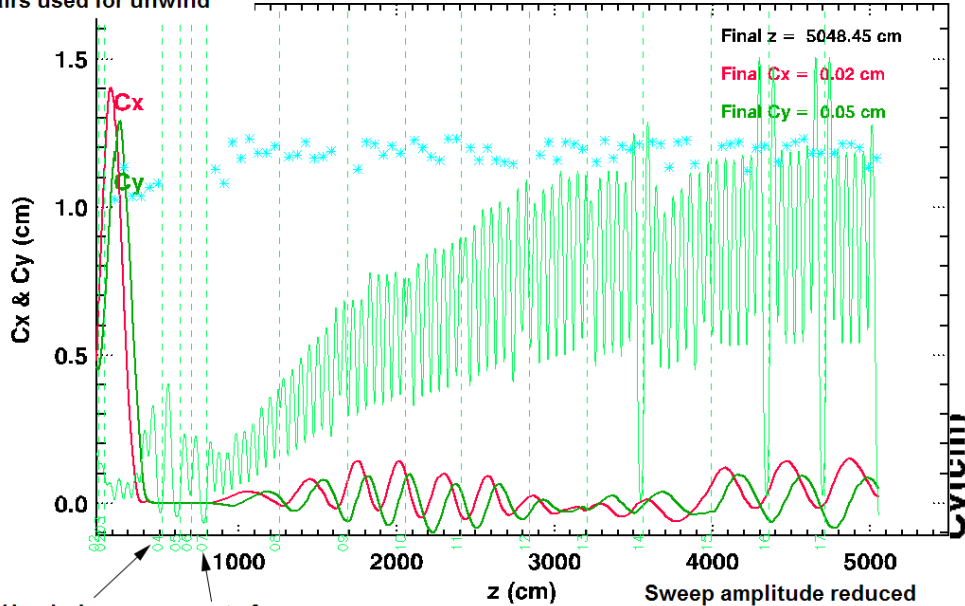
At the LIA exit, the phase position of the beam is a function of the accelerating cell potential -- fluctuations in cell pulsed-power voltage cause beam motion at the LIA exit.

- Both phase and gyro-radius are functions of accelerating gradient.
- The figure shows beam position at the exit as a function of percentage variations in cell accelerating potentials through the accelerator.



We significantly reduce the size of the helix by steering through the injector cells with dipole magnets.

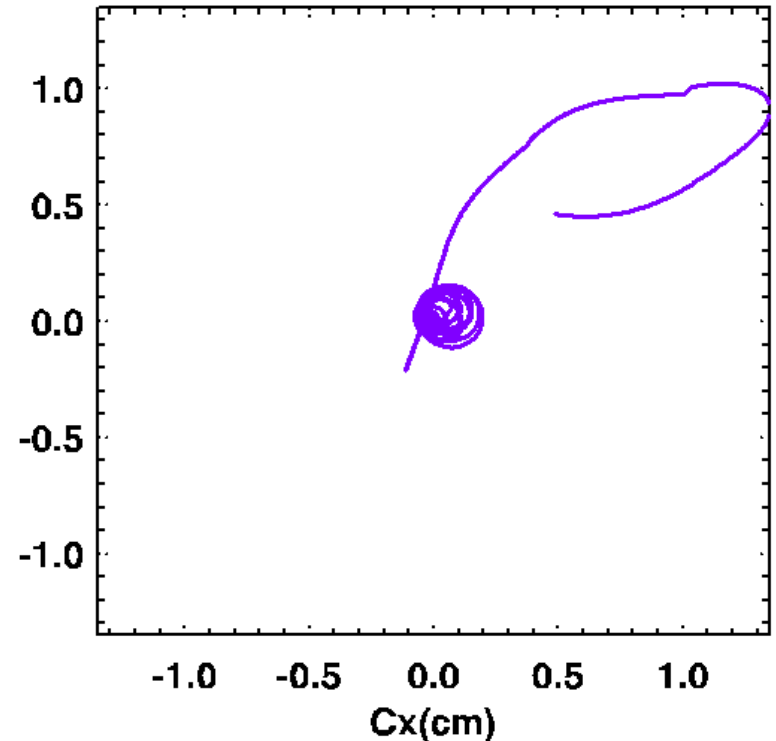
4 injector steering dipole pairs used for unwind



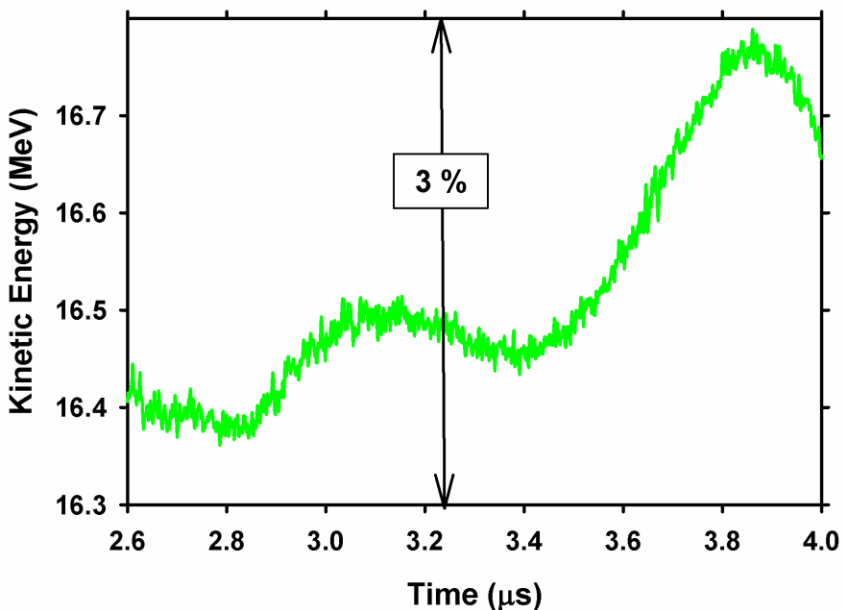
Unwind measurements from BPM04 and BPM07

Residual helical trajectory is the result of slight cell misalignments

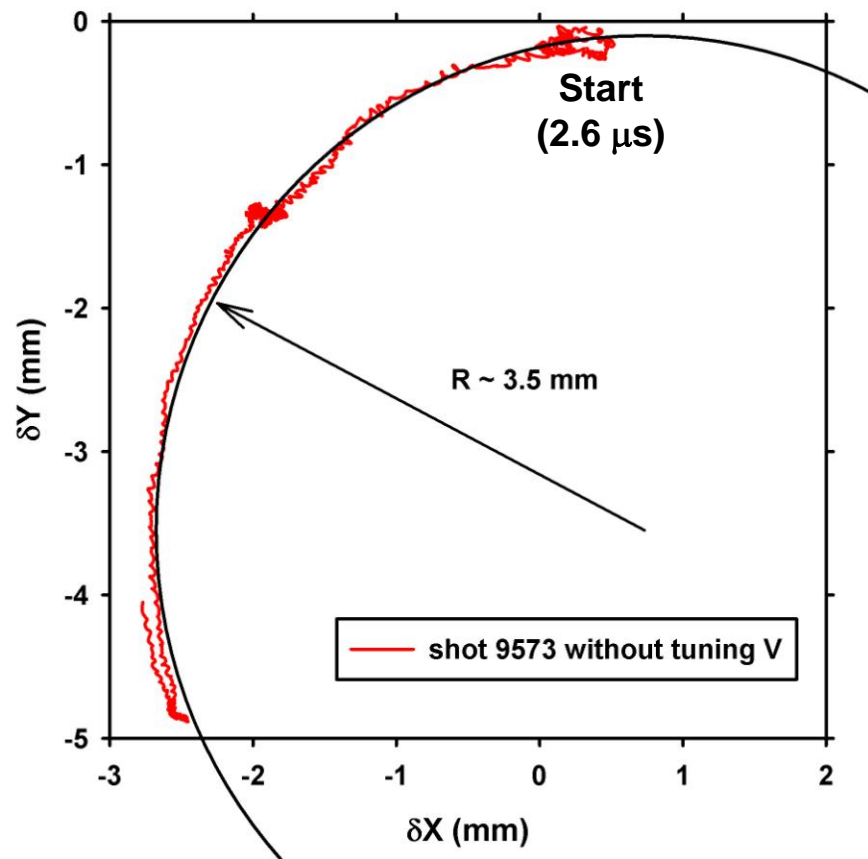
(rms offset ~ 3 mil; rms tilt ~ 0.3 mr)



As the cell voltages vary in time, so does the beam kinetic energy. So, the helix phase and gyro-radius vary at the accelerator exit, causing the beam to have a sweep in time.



Measured beam kinetic energy varies by more than 1% during the flat-top

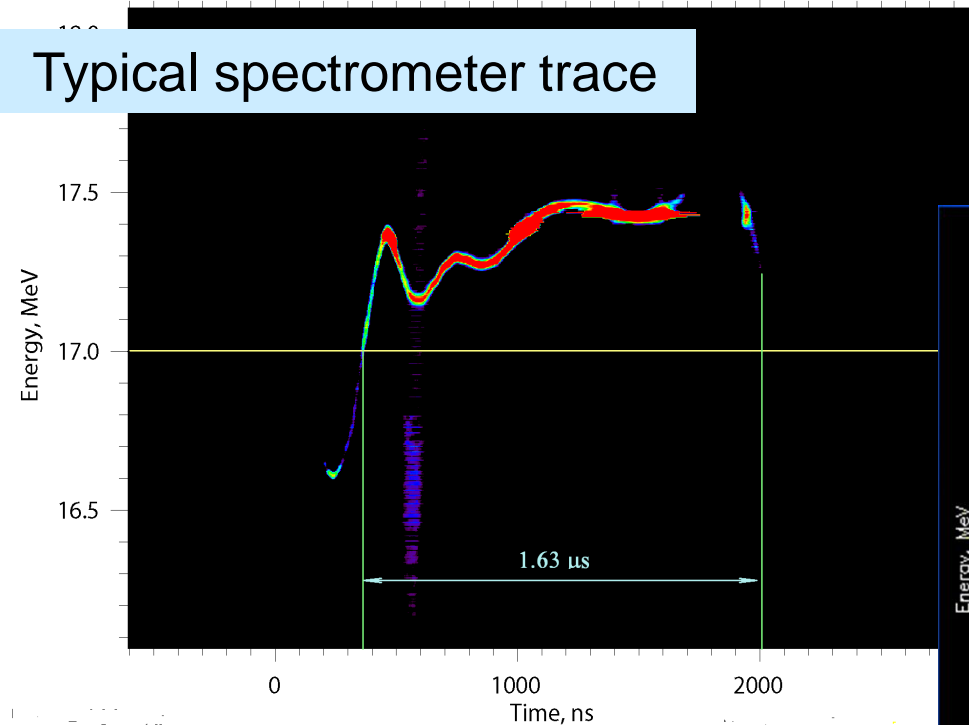


This energy variation causes a beam sweep at the accelerator exit.

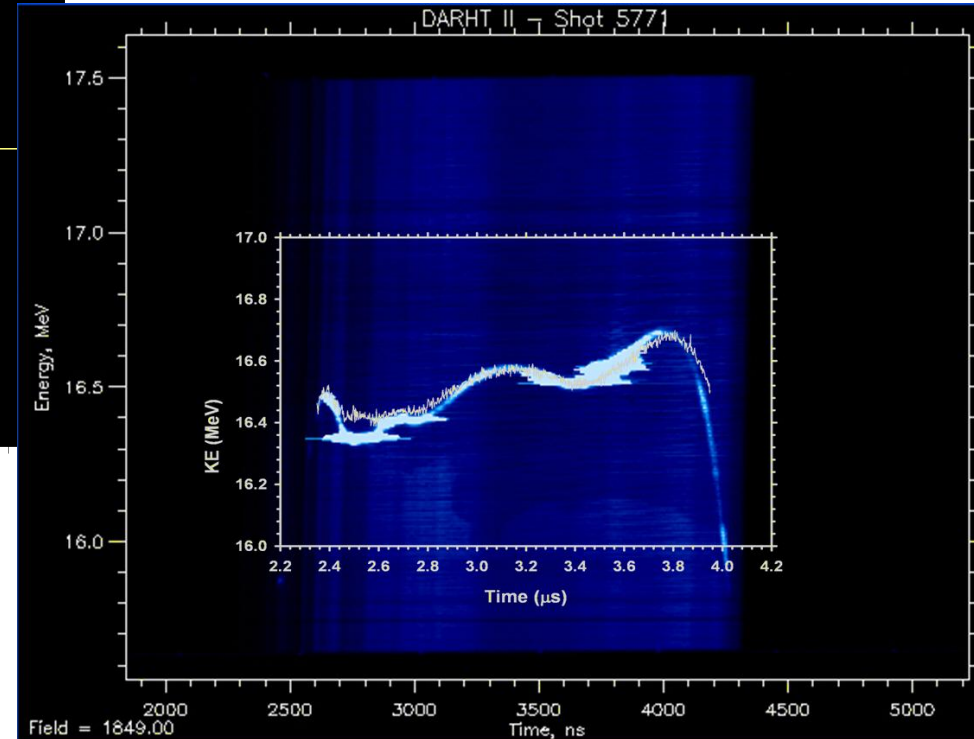
We measured the beam energy with magnetic spectrometer, calibrated to better than $\pm 0.5\%$ absolute, and then cross-calibrated our cell voltage monitors. These monitors now provide accurate beam energy measurements on every shot.

DARHT II - Shot 5733

Typical spectrometer trace

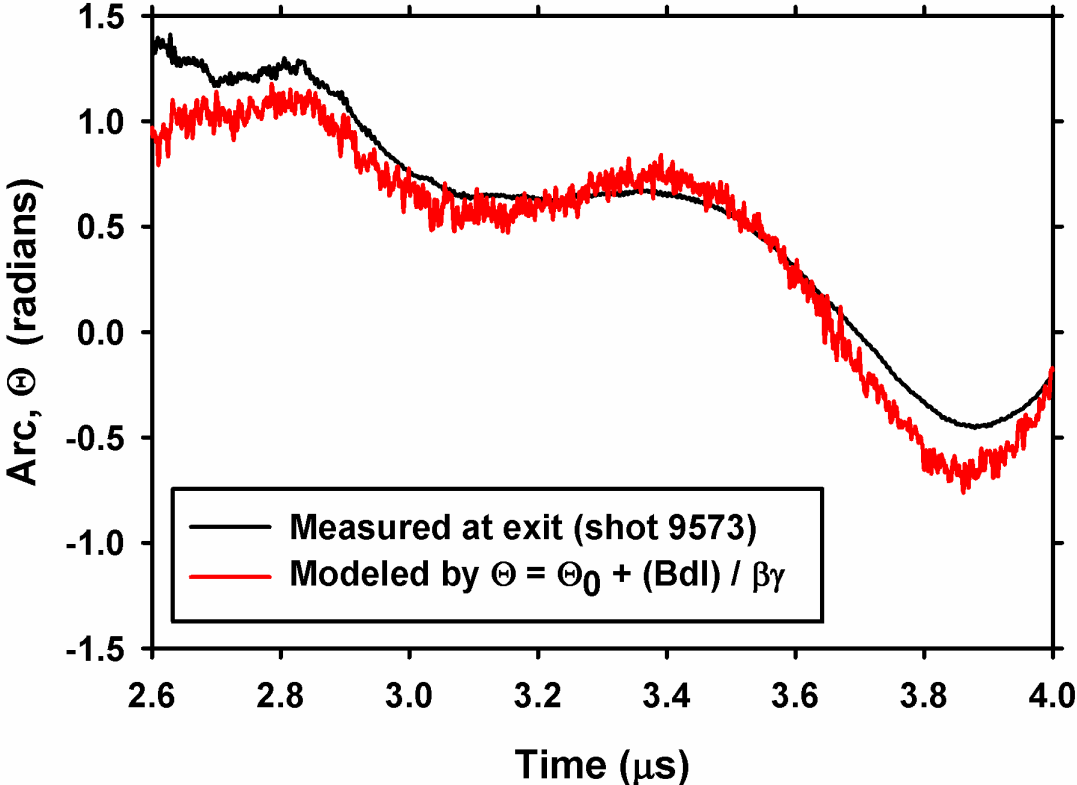


DARHT II - Shot 5771



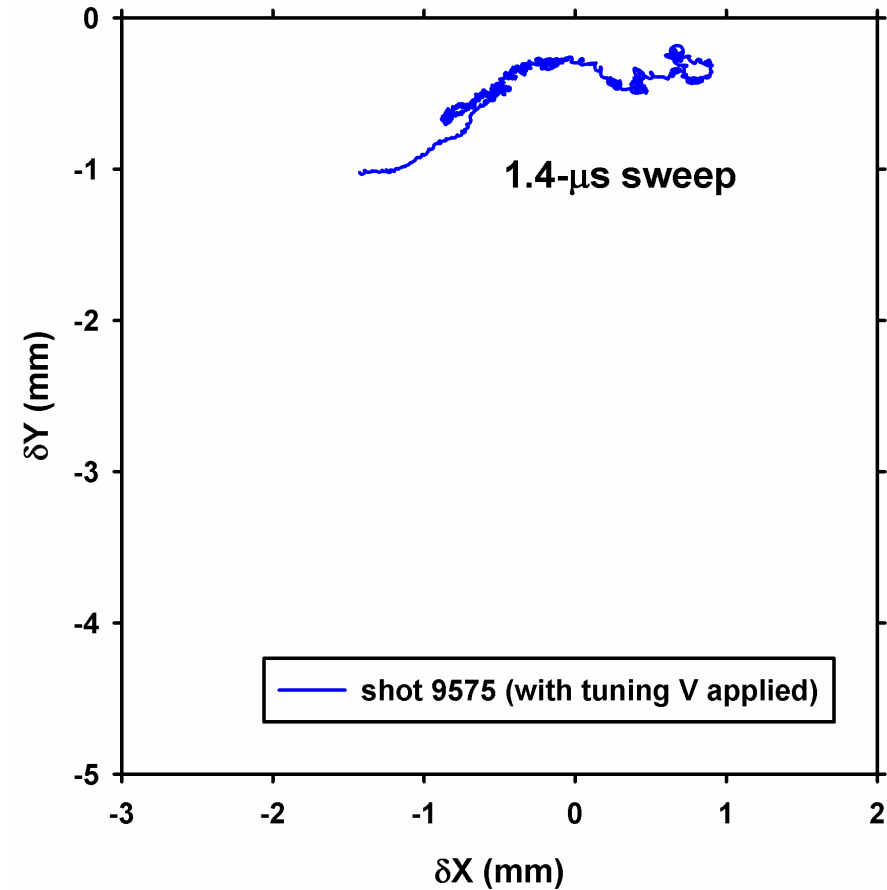
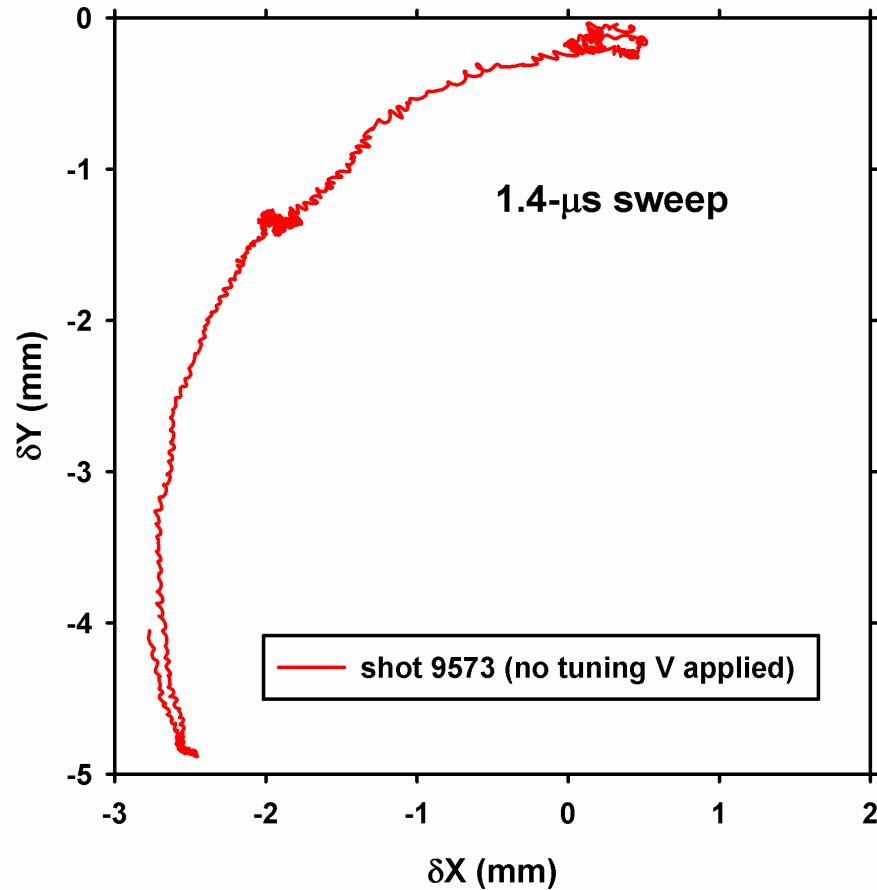
Cross-calibrated cell-monitor sum over-lay

The motion of the beam can be correlated with a model of a single, distributed-dipole deflection that is based on the measured beam energy. This suggests that a few corrector dipoles might cancel the motion.

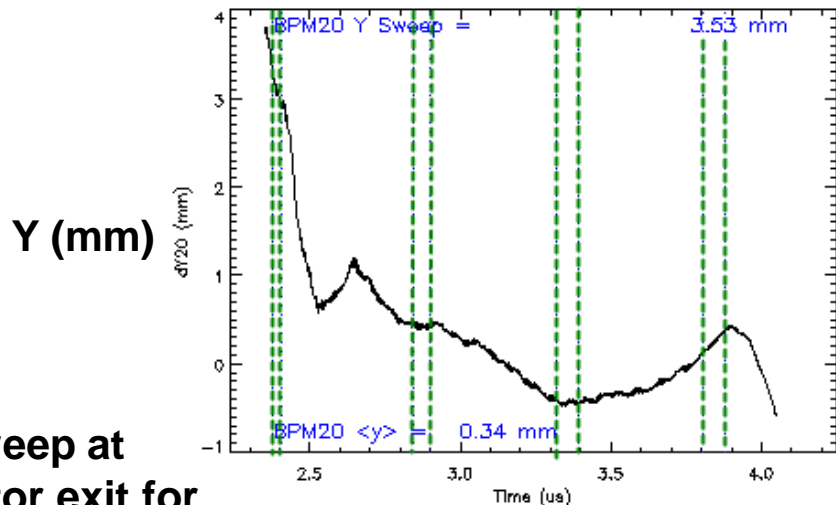


The single-dipole deflection model of energy dependence suggests that the sweep can be corrected with only one or two compensating dipoles.

We significantly reduced the sweep by varying selected corrector dipoles in the accelerator using the “Tuning V” procedure, first used on the ETA accelerator at Livermore .



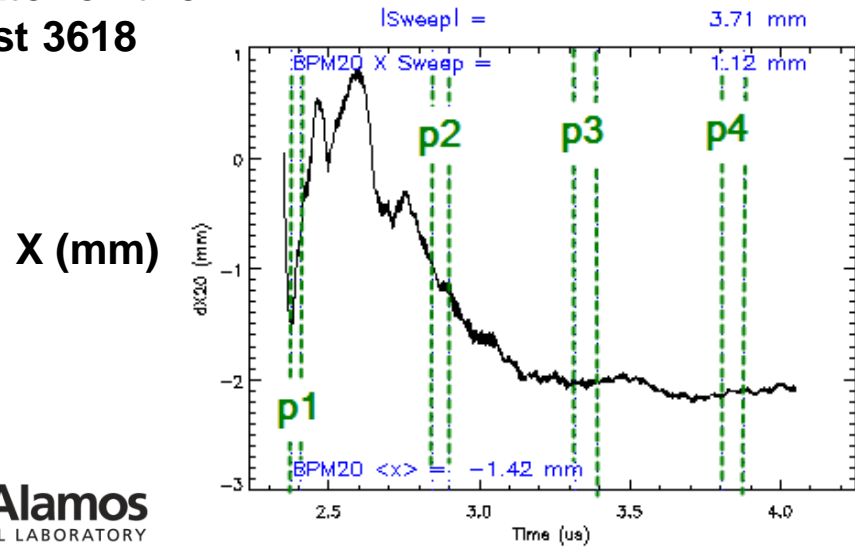
The sweep during the radiography pulses has been reduced by replacing defective solenoids, retuning, and judicious selection of pulse timing.



Beam sweep at accelerator exit for hydrotest 3618

Sweep at accelerator exit for hydrotests:

1. 3618 (4 pulses) : 3.7 mm
2. 3648 (4 pulses) : 1.6 mm



[Beam envelope simulations predict beam radius ~ 5 – 10 mm at exit]

Summary

- **We have attacked the problem of beam motion in the accelerator that would be detrimental to hydrotest radiography.**
- **We routinely measure beam motion at the accelerator exit :**
 - **Sweep has now been reduced to less than 30% of the beam envelope radius.**
 - **BBU has been reduced to less than 2% of the beam envelope radius.**
 - **Motion from other instabilities was not measurable.**
- **We have a good understanding of the causes of motion, so we can make further improvements, if required.**

Acknowledgement:

The unique achievements of the DARHT axis-2 accelerator are the result of a team effort by many dedicated people.

E. O. Abeyta, P. Aragon, R. Archuleta, G. Cook, D. Dalmas, Carl Ekdahl, K. Esquibel, R. Gallegos, R. Garnett, J. Harrison, J. Johnson, E. Jacquez, B. Trent McCuistian, N. Montoya, S. Nath, K. Nielsen, D. Oro, T. Priestley, M. Reed, C. Rose, M. Sanchez, M. Schauer, M. Schulze, G. Seitz, H. V. Smith, and R. Temple
Los Alamos National Laboratory, Los Alamos, NM 87545, USA

R. Anaya, G. Caporaso, F. Chambers, Y. J. Chen, S. Falabella, G. Guethlein, B. Raymond, R. Richardson, R. Scarpetti, J. Watson, and J. Weir
Lawrence Livermore National Laboratory, Livermore, CA 94550, USA

H. Bender, W. Broste, C. Carlson, D. Frayer, D. Johnson, C. Y. Tom, C. Trainham, and J. Williams,
NSTec, Los Alamos, NM 87544, USA

B. Prichard
SAIC, San Diego, CA 92121, USA

T. Genoni, T. Hughes, and C. Thoma,
Voss Scientific, Albuquerque, NM 87108, USA

Stanley Humphries, Jr.
Field Precision, Albuquerque, NM 87192, USA